Geomechanics and Engineering, *Vol. 36, No. 2 (2024) 121-130*
https://doi.org/10.12989/gae.2024.36.2.121

Damage evolution of red-bed soft rock: Progressive change from meso-texture to macro-deformation

Guangjun Cui[1,2], Cuiying Zhou[*2], Zhen Liu[**2] and Lihai Zhang[3]

[1]*Institute of Estuarine and Coastal Research/Guangdong Provincial Engineering Research Center of Coasts, Islands and Reefs, School of Ocean Engineering and Technology, Sun Yat-sen University, Guangzhou 510275, China*
[2]*Guangdong Engineering Research Centre for Major Infrastructure Safety, Sun Yat-sen University, Guangzhou 510275, China*
[3]*Department of Infrastructure Engineering, The University of Melbourne, Melbourne VIC 3010, Australia*

(*Received September 24, 2022, Revised November 15, 2023, Accepted December 6, 2023*)

Abstract. Many foundation projects are built on red-bed soft rocks, and the damage evolution of this kind of rocks affects the safety of these projects. At present, there is insufficient research on the damage evolution of red-bed soft rocks, especially the progressive process from mesoscopic texture change to macroscopic elastoplastic deformation. Therefore, based on the dual-porosity characteristics of pores and fissures in soft rock, we adopted a cellular automata model to simulate the propagation of these voids in soft rocks under an external load. Further, we established a macro–mesoscopic damage model of red-bed soft rocks, and its reliability was verified by tests. The results indicate that the relationship between the number and voids size conformed to a quartic polynomial, whereas the relationship between the damage variable and damage porosity conformed to a logistic curve. The damage porosity was affected by dual-porosity parameters such as the fractal dimension of pores and fissures. We verified the reliability of the model by comparing the test results with an established damage model. Our research results described the progressive process from mesoscopic texture change to macroscopic elastoplastic deformation and provided a theoretical basis for the damage evolution of these rocks.

Keywords: damage evolution; elastoplastic deformation; fissures; pores; red-bed soft rocks

1. Introduction

Red-bed, defined as rocks that have generally higher contents of hematite and are red in appearance, are the most widely distributed formations in South China. Most infrastructure projects in South China (e.g., expressways, tunnels, and bridges) are built on red-bed, especially red-bed soft rocks such as mudstone and sandstone (Liu *et al.* 2020, Xie *et al.* 2021, Zhou *et al.* 2021). Initially, these red-bed soft rocks were considered strong enough to meet engineering requirements. However, South China is a tropical–subtropical region that experiences high annual temperatures and rainfall (Fischer *et al.* 2012, Chen and Luo 2018). Once the red-bed soft rocks are excavated, they will be damaged in the external environment and their mechanical strength will decrease, gradually affecting the safety of infrastructure (Margherita *et al.* 2018, Zhou *et al.* 2020). Therefore, research on the damage evolution of red-bed soft rocks becomes important to engineering practices.

Damage evolution of red-bed soft rocks is a process of change of macroscopic mechanical properties caused by voids (mesoscopic pores and fissures, etc.) of mesoscopic texture under external load and environment (Bruning *et al.* 2018, Li *et al.* 2018a, Zhang *et al.* 2020). At present, there are many studies on rock damage evolution (Zhou and Zhu 2010, Liu *et al.* 2014, Wang *et al.* 2020a, Wang *et al.* 2020b). For example, Xie *et al.* (2011) and Chen *et al.* (2019) studied the damage evolution mechanism of hard rocks such as biotite granite or soft rocks such as mudstone from the perspective of energy conversion through cyclic loading and unloading tests or uniaxial/triaxial compression tests. Liu *et al.* (2017) established the functional relationship between damage variables and time by introducing Kachanov creep damage rate, obtained the nonlinear creep damage constitutive model of soft rocks, and studied the creep damage characteristics of mica-quartz schist. Based on the nonlinear damage creep characteristics of rock and damage variable, Ping *et al.* (2016) used the improved Burgers model, Hooke model and St. Venant model to define the nonlinear damage creep constitutive model of high stress soft rocks. However, the research on the damage evolution of red-bed soft rocks is limited, especially the progressive process from mesoscopic texture change to macroscopic elastoplastic deformation, which is difficult for the safe construction and operation of soft rock engineering (Zhang and Cai 2010). Of course, there are also studies involving the changes of mesoscopic texture. For example, Nejati and Ghazvinian (2014) studied the effect of brittleness on the fatigue damage evolution of onyx marble, sandstone and soft limestone, and studied the propagation of mesoscopic voids using acoustic emission (AE) technology. Wang *et al.* (2022) conducted a series of uniaxial compression AE tests on hollow red sandstone and

*Corresponding author, Professor
E-mail: zhoucy@mail.sysu.edu.cn
**Corresponding author, Associate Professor
E-mail: liuzh8@mail.sysu.edu.cn

ISSN: 2005-307X (Print), 2092-6219 (Online)

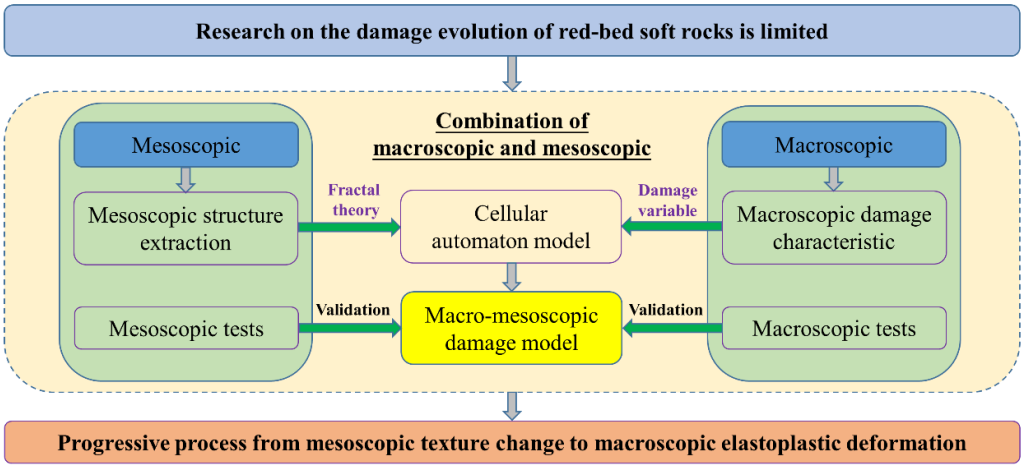

Fig. 1 Block diagram illustrating the steps involved in this study

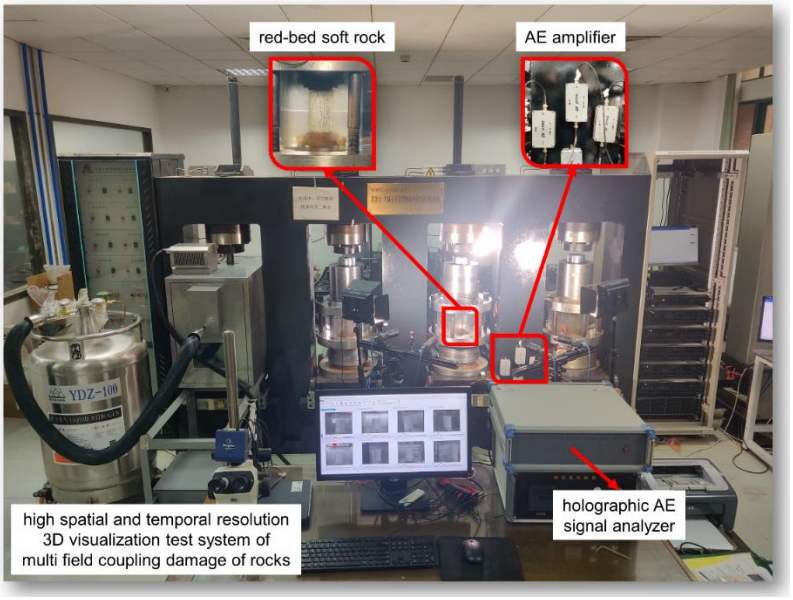

Fig. 2 Testing equipment

granite with different bore diameters, and established a damage constitutive model based on the AE ring count. But they did not establish a damage evolution relationship between the change of mesoscopic texture and macroscopic elastoplastic deformation.

Therefore, in order to study the damage evolution of red-bed soft rocks from the perspective of the progressive process of mesoscopic texture change to macroscopic elastoplastic deformation, the mesoscopic texture of the sample was extracted first, and then the change of mesoscopic texture in the process of macroscopic elastoplastic deformation of the sample was calculated by cellular automata model, which was correlated with the macroscopic damage model to obtain the macroscopic-mesoscopic damage model of red-bed soft rocks. Finally, the reliability of the model was verified by macroscopic and mesoscopic tests, and the progressive process from mesoscopic texture change to macroscopic elastoplastic deformation of red-bed soft rocks was explained.

2. Methods

The study contents, methods, and steps are shown in Fig. 1.

2.1 Macroscopic and mesoscopic tests

This study includes macroscopic test (uniaxial compression test) and mesoscopic tests (AE test and scanning electron microscope (SEM) test). The SEM test data is mainly used for the identification and feature extraction of the mesoscopic texture of red-bed soft rocks. Uniaxial compression test and AE test are carried out simultaneously, and the data are used to verify the macroscopic and mesoscopic damage evolution model of red-bed soft rocks.

2.2 Identification and feature extraction of mesoscopic texture

Rock is one of the dual media of pores and fissures. This kind of medium is composed of solid particles, pores and fissures (Elsworth and Bai 2020). Pore space and fissure space together constitute the void space in the medium. These void spaces have a great impact on the mesoscopic texture changes of red-bed soft rocks under the action of the external environment (Benavente *et al.* 2007, Liu *et al.* 2021). Therefore, in order to study the mesoscopic texture changes of red-bed soft rocks, it is necessary to identify pores and fissures respectively and extract their characteristics from SEM images. In this study, we defined the mesoscopic scale as <100 μm with pores generally <2 μm and fissures generally 2~100 μm. Firstly, in order to reduce the noise of the image, the image is subjected to grayscale (Wei *et al.* 2014) and binarization (Liang 2016) processing before quantitative analysis. In gray and binary image processing, the particles and voids (pores and fissures) in the images were distinguished. To further discern the pores and fissures, we set a reasonable threshold (pixel size of the voids) in a binarization image to distinguish between pores and fissures in the same way that particles and voids were determined.

Fractal theory was then used to extract the mesoscopic texture characteristics of the red-bed soft rocks. Fractal is a new type of geometry and is mainly used to describe irregular objects. It can be treated as the geometric abstraction of a natural form. A fractal dimension is a quantitative characterization and basic fractal parameter, including topological, hausdorff, and box dimensions (Li *et al.* 2018b, Wu *et al.* 2018). Commonly used theoretical methods for determining a fractal dimension include the radius of gyration, Sandbox, density correlation function, and box dimension (Zhao *et al.* 2017). In this study, we used the box dimension method to extract pores and fissures characteristics.

The basic idea of the box dimension method is to assume that an image of pixels $L \times L$ is divided into an orthogonal grid of size $(L/a) \times (L/a)$ by a square with side length a. The total number of grids with pores and fissures in the grid is counted as $N_p(a)$. If we change a so that it serializes within the range a_1, a_2, a_3,... a_n, then the corresponding sequence values $N_p(a_1)$, $N_p(a_2)$, $N_p(a_3)$,... $N_p(a_n)$ and the corresponding relationship of $\ln a$ to $\ln N_p(a)$ can be intuitively determined by depicting the two groups of data in a double logarithmic coordinate system. If the relationship is linear, it indicates that the distribution of pores and fissures has fractal characteristics. If the slope of the straight line fitted by the least squares method is k, then the fractal dimension of voids can be determined by the following equatio

$$D_{pf} = -k \tag{1}$$

where, D_{pf} is the fractal dimension of pores and fissures, and k is the slope of the straight line of $\ln a$ – $\ln N_p(a)$. The fractal dimension of pores (D_p) and fissures (D_f) were also obtained by analyzing the image of pores and fissures after separation.

2.3 Damage variable and elastoplastic damage model

Soft rock deformation consists of elastic and plastic stages. Damage in the plastic phase manifests because of the initiation, expansion, and penetration of mesoscopic pores and fissures (Abd Rahman *et al.* 2018). Lemaître and Chaboche (1990) suggested that the damage variable was the ratio of the void area to the total area

$$D = 1 - \frac{A^*}{A} \tag{2}$$

where, D is the damage variable, A^* is the effective resisting area, and A is the overall area. The condition depends on the state of the damage variable. When $D = 0$, there is a non-destructive state, when $D = 1$, it is a completely damaged state, and when $0 < D < 1$, it reflects a partially damaged state.

Damage to red-bed soft rocks is mainly caused by the initiation and growth of mesoscopic pores and fissures (Aubertin and Simon 1997). At this scale, the rocks are discontinuous. In most engineering materials, these voids are considered spatially and are randomly distributed in all directions. The damage variable can solve this discontinuity so that the material is then regarded as an isotropic medium. Assuming our soft rock is subjected to isotropic damage; the effective stress would increase with a decrease in the effective bearing area due to damage. Based on the strain equivalence hypothesis (Lemaître and Chaboche 1990), the deformation behavior of a damaged rock can be reflected by the change in effective stress. The effective stress tensor can be expressed as

$$\tilde{\boldsymbol{\sigma}}_{\boldsymbol{ij}} = \frac{\boldsymbol{\sigma}_{\boldsymbol{ij}}}{1 - D} \tag{3}$$

where, $\tilde{\boldsymbol{\sigma}}_{\boldsymbol{ij}}$ is the effective stress tensor and $\boldsymbol{\sigma}_{\boldsymbol{ij}}$ is the stress tensor.

Assuming the soft rock is isotropic before damage, the flexibility matrix can be expressed as

$$[\boldsymbol{C^{-1}}] = \frac{1}{E}\begin{bmatrix} 1 & -\nu & -\nu & 0 & 0 & 0 \\ -\nu & 1 & -\nu & 0 & 0 & 0 \\ -\nu & -\nu & 1 & 0 & 0 & 0 \\ 0 & 0 & 0 & 2(1+\nu) & 0 & 0 \\ 0 & 0 & 0 & 0 & 2(1+\nu) & 0 \\ 0 & 0 & 0 & 0 & 0 & 2(1+\nu) \end{bmatrix} \tag{4}$$

where, E is the elastic modulus and ν is Poisson's ratio.

According to the equivalent strain principle (Zhang and Cai 2010), the isotropic damaged soft rock $[\boldsymbol{C^{-1}}]$ can be expressed as

$$\begin{aligned} [\tilde{\boldsymbol{C}}^{-1}] &= \frac{1}{(1-D)^2}[\boldsymbol{C^{-1}}] \\ &= \frac{1}{(1-D)^2 E}\begin{bmatrix} 1 & -\nu & -\nu & 0 & 0 & 0 \\ -\nu & 1 & -\nu & 0 & 0 & 0 \\ -\nu & -\nu & 1 & 0 & 0 & 0 \\ 0 & 0 & 0 & 2(1+\nu) & 0 & 0 \\ 0 & 0 & 0 & 0 & 2(1+\nu) & 0 \\ 0 & 0 & 0 & 0 & 0 & 2(1+\nu) \end{bmatrix} \end{aligned} \tag{5}$$

The stress–strain increment form of the elastoplastic damage is provided as

$$d\sigma_{ij} = \tilde{C}_{ijkl}\left(d\varepsilon_{kl} - d\varepsilon_{kl}^{p}\right) - \tilde{C}_{ijkl}\left(\varepsilon_{kl} - \varepsilon_{kl}^{p}\right)d\Omega \tag{6}$$

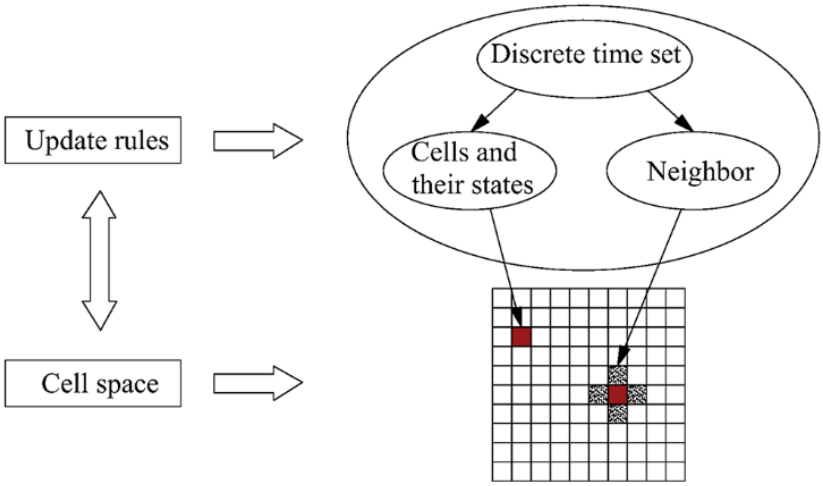

Fig. 3 Schematic diagram of a cellular automata simulation

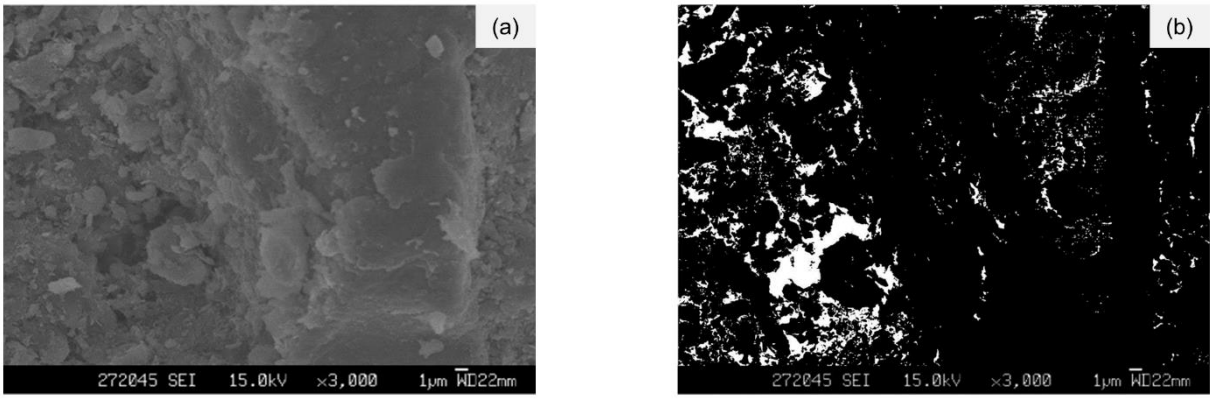

(a) Original image (b) image after grayscale and binarization processing

Fig. 4 SEM image processing results. The black areas in (b) show particles and the white areas show pores and fissures

where, $\tilde{C}_{ijkl}$ is the effective stiffness matrix.

Then, Eq. (6) can be rewritten as

$$\begin{aligned} d\varepsilon_{ij} &= \tilde{C}_{ijkl}^{-1} d\sigma_{kl} - \tilde{C}_{ijkl}^{-1} d\tilde{C}_{ijkl}\left(\varepsilon_{ij} - \varepsilon_{ij}^{p}\right) + d\varepsilon_{ij}^{p} \\ &= \tilde{C}_{ijkl}^{-1} d\sigma_{kl} + d\tilde{C}_{ijkl}^{-1}\sigma_{kl} + d\varepsilon_{ij}^{p} \\ &= \tilde{C}_{ijkl}^{-1} d\sigma_{kl} + \frac{\partial \tilde{C}_{ijkl}^{-1}}{\partial D} dD\sigma_{kl} + d\varepsilon_{ij}^{p} \end{aligned} \tag{7}$$

where, $\tilde{C}_{ijkl}^{-1} d\sigma_{kl}$ represents the strain increment due to elastic deformation, $\frac{\partial \tilde{C}_{ijkl}^{-1}}{\partial D} dD\sigma_{kl}$ represents the increment of damage, and $d\varepsilon_{ij}^{p}$ represents the strain increment due to plastic deformation. Therefore, the total strain of soft rock elastoplastic deformation consists of three increments: elastic, damage, and plastic.

2.4 Cellular automata model of the soft rock mesoscopic texture change

A cellular automata is a mathematical model for describing the overall evolution of a discrete dynamic system under random initial conditions by developing mathematical rules (Pan *et al.* 2015, Yan *et al.* 2018) and has been widely applied in various fields (Nishiyama *et al.* 2014, An *et al.* 2019). The self-replication, chaos, and other characteristics of a cellular automata often lead the spatial configurations of cellular automata models to show similar fractal characteristics. Thus, complex fractal phenomena can be simulated by cellular automata (Yan *et al.* 2014). The relationship between cellular automata and fractal dimension theory can simulate the energy change during soft rock damage. There are four components in a cellular automata model: cell, cell space, neighbor, and local rule (Fig. 3).

Assuming r is the radius of the cell neighbor and Z is the set of integers, the change in the state of cells over time t based on the overall evolution F can be expressed as

$$F : S_Z^t \to S_Z^{t+1} \tag{8}$$

where, S_Z is the distribution of state S in integer set Z, and F is the complex dynamic evolution that is determined by the local evolution rule f of each cell. For a one-dimensional space, the cell and its neighbors can be described as S_{2r+1}, and the local function can be denoted as

$$F(S_i^{t+1}) = f(S_{i-r}^t, \cdots, S_i^t, \cdots S_{i+r}^t) \tag{9}$$

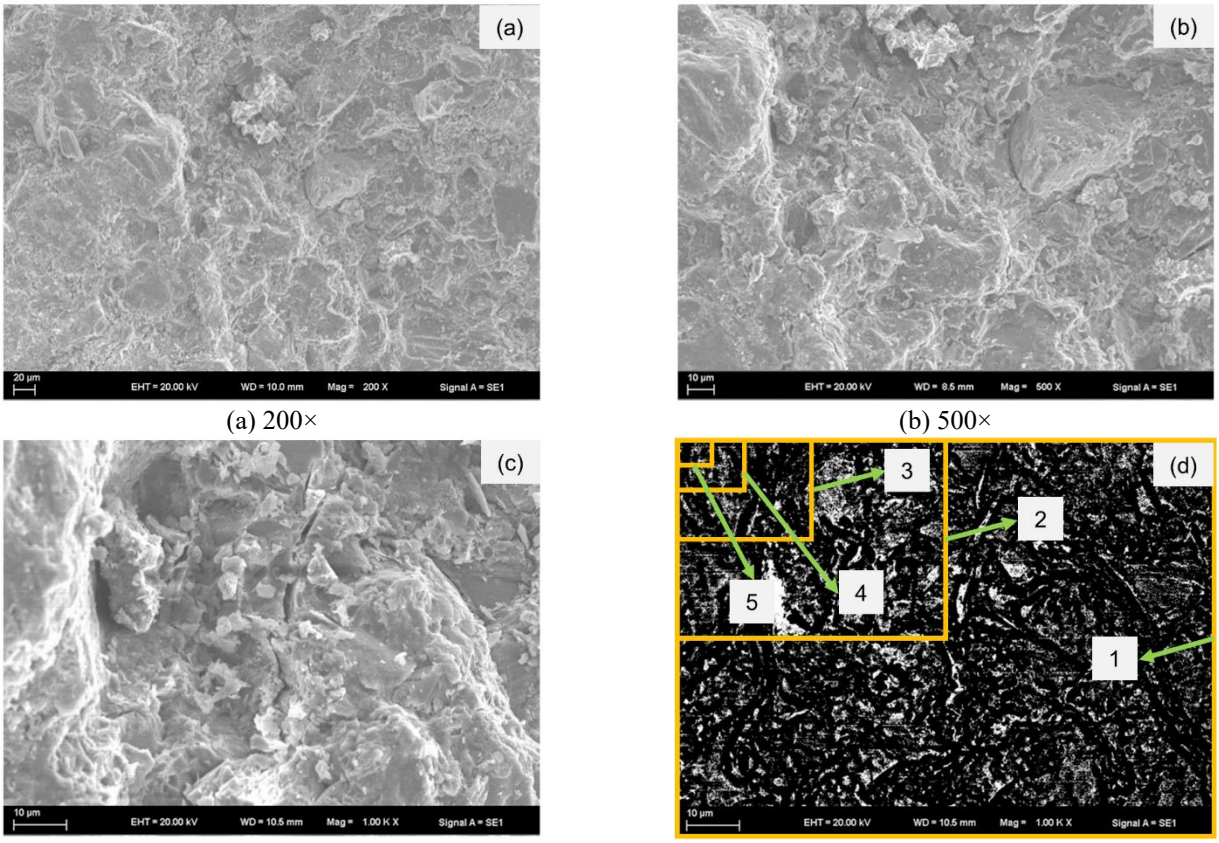

(a) 200× (b) 500×

(c) 1,000× (d) pores and fissures statistical method

Fig. 5 SEM images of the red-bed soft rocks at different magnifications

where, S_i^t represents the state of the cell at position i at time t.

3. Results and discussion

In this section, firstly, red-bed soft rock's mesoscopic textures were quantitatively characterized by identifying the pores, fissures, and particles. Then, based on the double porosity theory, the damage evolution of red-bed soft rocks was described, the relationship between damage variables and mesoscopic texture was established, and the macroscopic-mesoscopic elastoplastic damage model was constructed. Finally, the model was validated by using test data.

3.1 Quantitative characterization of red-bed soft rock's mesoscopic textures

The voids of red-bed soft rocks, containing pores and fissures, in the SEM images can be clearly distinguished (Fig. 4). To further distinguish the pores and fissures, the binary images were processed using morphological methods. Fig. 5 shows multiple SEM images at different magnifications from the same area of a sample. There are many studies on the process of calculating pores and fissures distribution by grid method (Zhao 2010). Firstly, the image with side length L is divided into a grid with side length of L (Fig. 5(d)). If the grid is occupied by pores or fissures, it is set to 0, otherwise it is set to 1. Then, the image with side length L is further divided into grids with side length of L/m, m is 2, 3, 4, ..., until the ratio of 0 to 1 in step i is equal to that in step $i+1$. At this time, a grid is a pixel. Finally, according to the connectivity of adjacent grid boundaries, the grids belonging to the same pores or fissures are combined, and the size and number of pores or fissures are calculated (Fig. 6, Eq. (10)).

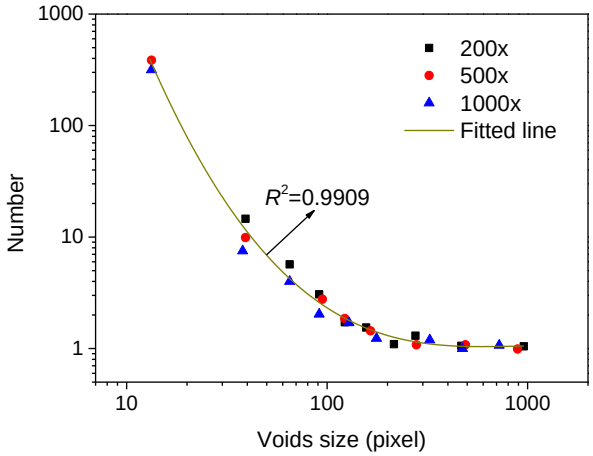

Fig. 6 Number of voids of different sizes

$$y = -0.035x^4 - 0.104x^3 + 2.682x^2 - 9.540x + 10.097 \quad (10)$$

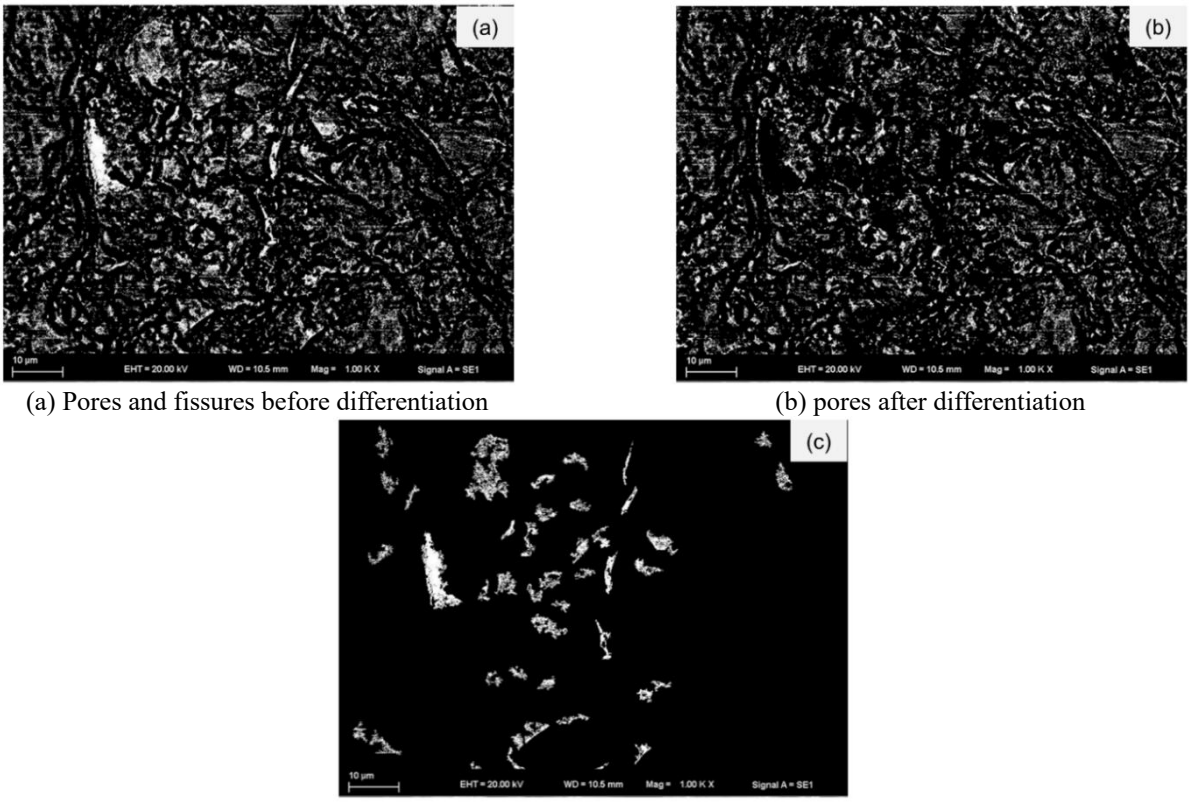

(a) Pores and fissures before differentiation (b) pores after differentiation

(c) fissures after differentiation

Fig. 7 Differentiation of pores and fissures in SEM images

By analyzing the statistical data in Fig. 6, we concluded that (1) the number of small-sized voids was larger than relatively large-sized voids, and (2) the sizes of red-bed soft rocks voids were similar regardless of scale.

Based on the derivative of Eq. (10), after trial calculation, we set a threshold of −1, which can better distinguish pores and fissures in the image (Fig. 7). Porosity n was then calculated using a ratio of the void area to total area. On this basis, the fractal dimension of pores and fissures was analyzed by the box dimension method. The statistical results are shown in Table 1.

3.2 Evolution of pores and fissures damage in red-bed soft rocks mesoscopic textures

By extracting information from the SEM images, we were able to extract the mesoscopic pores and fissures information by using pixel points to reconstruct a damage model. Similarly, a two-dimensional grid was used to characterize the pores and fissures (Fig. 8). When a two-dimensional grid represents voids, the fractal geometry distribution and grid scale are

$$N_a = N_0 \cdot a^{-D_f} \tag{11}$$

where, N_a is the degree of disorder in void distribution corresponding to grid scale a, N_0 is the initial distribution of the fissures, and D_f is the fractal dimension of the fissures. Here, the fractal dimension of pores D_p can be substituted for D_f to obtain a similar expression for the degree of disorder in the void distribution. We note that some other interpretations of Eq. (11) can be found in (Bour *et al.* 2002). In practice, a is generally a fixed value. Then, the fissures distribution degree of disorder N_a is only

Table 1 Mesoscopic texture parameters extracted from binary images of the different red-bed soft rocks samples

Sample number	Pores and fissures (%)	Pore fractal dimension	Fissure fractal dimension
1	13.2	0.66	1.21
2	16.6	0.75	1.29
3	13.7	0.68	1.29
4	14.8	0.75	1.14
5	13.1	0.70	1.24
6	16.9	0.62	1.25
7	13.2	0.61	1.24
8	14.4	0.65	1.25
9	14.2	0.76	1.27
10	16.8	0.68	1.11
11	15.0	0.58	1.30
12	14.6	0.62	1.29
13	15.2	0.84	1.09
14	14.8	0.78	1.29
15	14.2	0.72	1.24
Average value	**14.7**	**0.69**	**1.23**

Note: "Pores and fissures (%)" is the ratio of the area of pores and fissures to total area

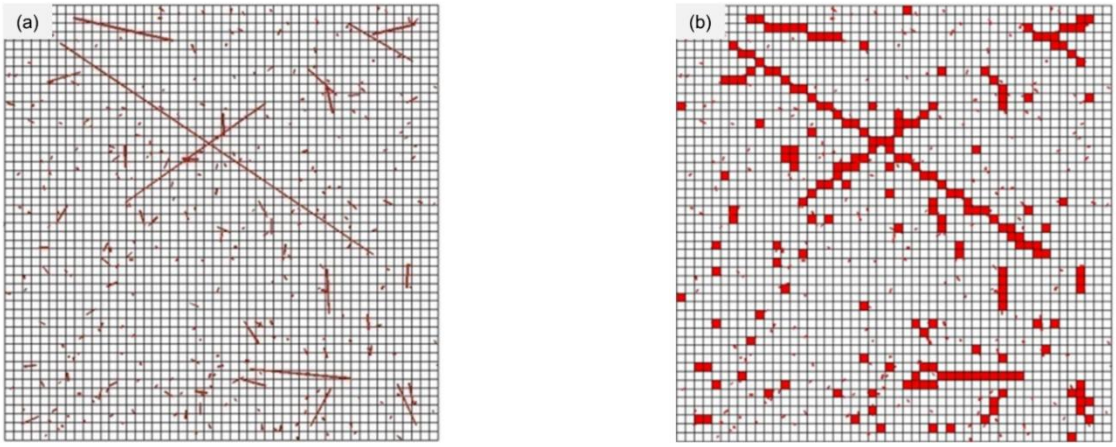

(a) original distribution space (b) a two-dimensional gridded distribution

Fig. 8 Voids distribution

Table 2 Fitting results for the initial and final values ($\boldsymbol{A_1}$ and $\boldsymbol{A_2}$, respectively), center ($\boldsymbol{x_0}$), and power of the curve ($\boldsymbol{p}$) that shows the relationship between damage porosity ($\boldsymbol{n}$) and damage variable ($\boldsymbol{D}$) *under various fissures distribution values (*$\boldsymbol{N_0}$)

Fitted parameter	$\boldsymbol{N_0 = 0.1}$	$\boldsymbol{N_0 = 0.2}$	$\boldsymbol{N_0 = 0.4}$	Average value	Variance
A_1	−0.019	−0.018	−0.018	−0.018	2.222E−7
A_2	1.141	1.223	1.127	1.164	1.793E−3
x_0	0.599	0.627	0.628	0.618	1.807E−4
p	3.345	2.946	3.978	3.423	0.181

related to the initial distribution value N_0 and fractal dimension D_f of the fissures. That is, N_a is a function of N_0 and D_f.

The damage evolution of red-bed soft rocks was analyzed by defining the damage variable and studying the fractal geometry of the disorder degree in mesoscopic voids distribution and the grid scale, combined with the cellular automata model. We used this procedure to study the relationship between porosity, the initial fissures distribution, the fractal dimension of fissures, and the damage variable.

Initially, we set the initial distribution value and fractal dimension of fissures, and studied the evolutionary relationship between simulated porosity and damage variable by changing the porosity (Fig. 9).

The functional relationship between the damage porosity and damage variable can be fitted with a logistic curve

$$D = A_2 + (A_1 - A_2) / (1 + (n / x_0)^p) \quad (12)$$

where, n is the damage porosity, D is the damage variable, and A_1, A_2, x_0 and x_0 are all fitted parameters corresponding to the initial value, final value, center, and power of the curve, respectively. The fitting results are shown in Table 2.

We determined that the initial values of the fissures distribution and fractal dimension had little influence on the relationship between the damage variable and damage porosity. However, the fractal dimension of fissures influenced the range or initial value of the damage porosity (Fig. 10). The relationship between the fractal dimension of fissures and the initial damage porosity conformed to a quadratic polynomial fitting equation, which had an indirect effect on the damage variable

$$n = B_3 + B_1 \cdot D_f + B_2 \cdot D_f^2 \quad (13)$$

where, B_1, B_2, and B_3 are all fitted parameters, equal to −2.153, 1.011, and 1.179, respectively.

By substituting Eq. (13) into Eq. (12) and then into the macroscopic damage model (Eqs. (6) or (7)), we obtained the damage model expressed by the mesoscopic texture parameters. In this way, we described the damage extent within mesoscopic damage mechanics and established the relationship between macroscopic deformation/damage and mesoscopic texture parameters.

3.3 Model validation

The model validation needs to be carried out from the macroscopic and mesoscopic scales. According to the macroscopic and mesoscopic damage evolution Eqs. (7), (11), (12), and (13), we selected 3 representative model verification parameters (initial fractal dimension D_f, initial distribution value N_0, and initial damage porosity n). Based on the previously developed rock fractal model (Zhao 2010, Zhang *et al.* 2019) and the mesoscopic test results: (1) with the average value of the initial fractal dimension D_f in Table 1 and the D_f value in Fig. 9, we finally obtained the fractal

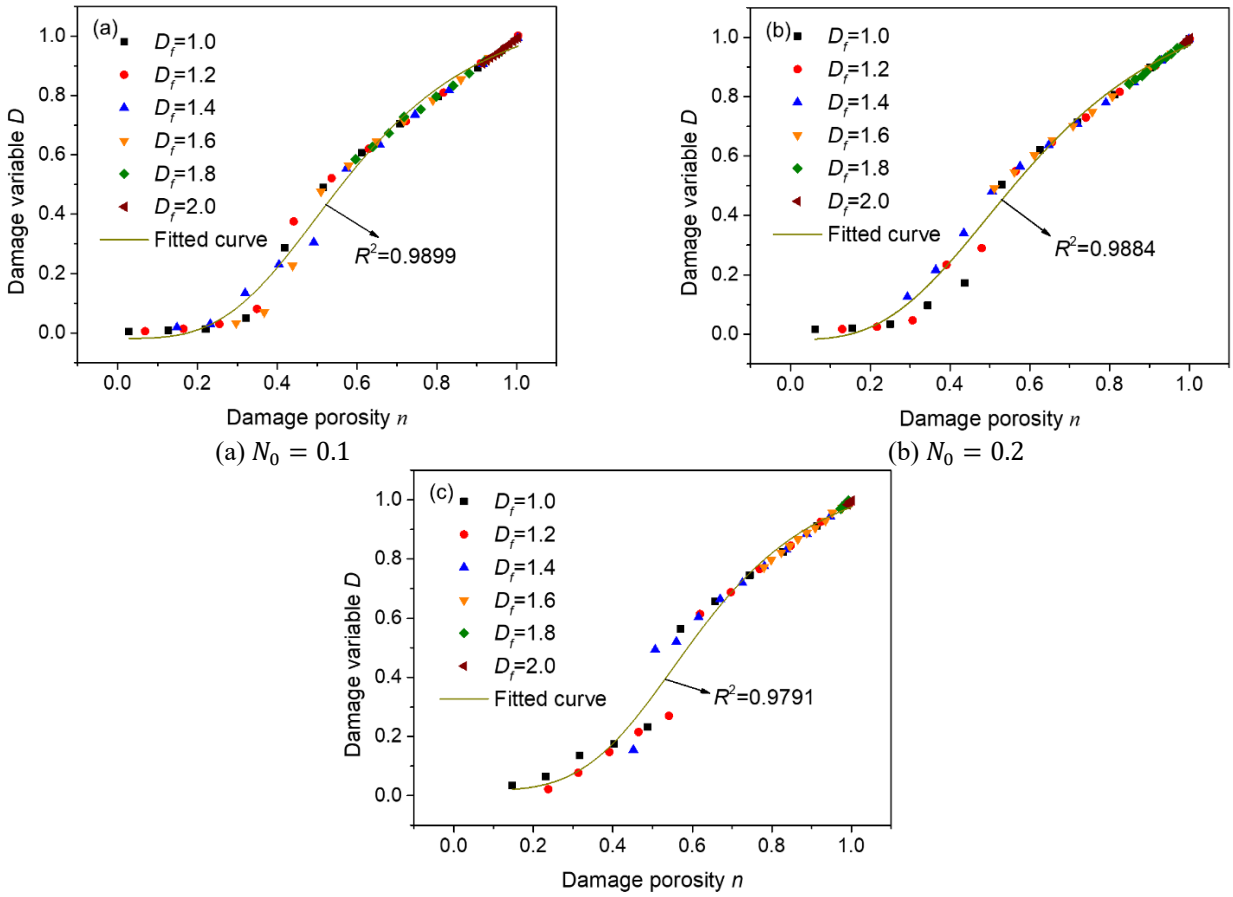

(a) $N_0 = 0.1$ (b) $N_0 = 0.2$

(c) $N_0 = 0.4$

Fig. 9 The damage variable D as a function of damage porosity n under various fractal dimensions of fissures D_f(1~2) and initial values of fissures distribution N_0

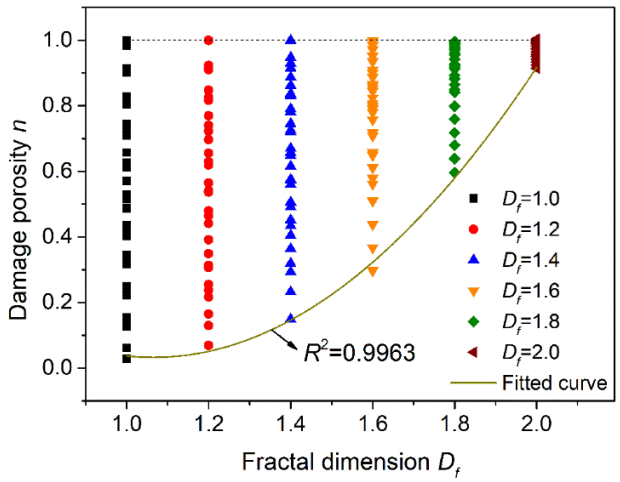

Fig. 10 Relationship between fractal dimension of fissures and damage porosity

dimension $D_f = 1.2$. (2) Since there are relatively few fissures in Fig. 7(c), we got the initial fissures distribution value $N_0 = 0.1$. (3) With the average proportion of pores and fissures in Table 1 and the initial damage porosity in Fig. 7 (the proportion of pores is larger than fissures) and Fig. 9, we selected the initial damage porosity n as 8.26%.

The rock damage was simulated with a cellular automata model to investigate the evolution of fissures. We formed a cellular space by treating a local mesoscopic image as a cell and other local images as neighbors of the cell. The elastoplastic model of soft rocks (Eq. (7)) was considered an update rule. The model size was 50 mm × 50 mm, which was divided into 2,500 cells. Fig. 11 shows the relationship between AE frequency and the loading step, as well as the relationship between damage variables, loading step, and axial strain. Fig. 12 shows the comparison of the theoretically predicted stress–strain curve with the test results.

From a mesoscopic point of view, higher AE frequencies lead to more rapid inter-particle fracturing within the rock, and as more mesoscopic voids were generated, the corresponding damage grew faster (Fig. 10). The highest AE frequency corresponds to the highest slope of the damage variable curve (Fig. 10). From the macroscopic point of view, the theoretical model and test data were consistent in terms of peak stress and peak strain, as well as the development and changes in the curve (Fig. 11). In order to facilitate comparison, the stress-strain curve in the test results is a representative curve that is closest to the average value of the test results among the five groups of test results. These results show that the theoretical predictions fit the test results reasonably well.

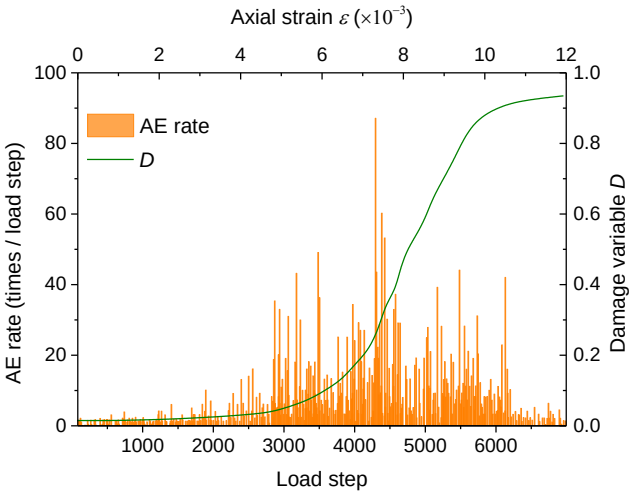

Fig. 11 AE rate and evolution of soft rock damage

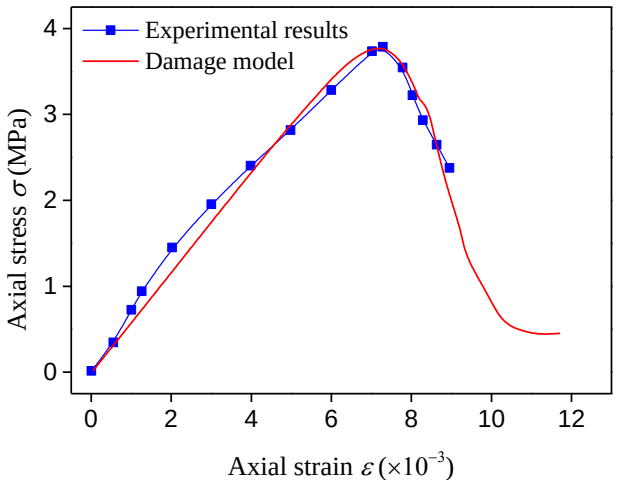

Fig. 12 Comparison of the theoretically predicated stress–strain curve with the test results

4. Conclusions

At present, the macroscopic-mesoscopic damage evolution of red-bed soft rocks is not clear, especially the progressive process from mesoscopic texture change to macroscopic elastoplastic deformation. In this study, we established the relationship between mesoscopic texture change and macroscopic elastoplastic deformation of red-bed soft rocks by studying their textural evolution coupled with a macroscopic damage model; the reliability of the model was verified by test data.

Our results indicate that the relationship between the number and voids size conformed to a quartic polynomial through mesoscopic textural feature extraction. The cellular automata model showed that the relationship between the damage variable and damage porosity conformed to a logistic curve, whereas the relationship between damage porosity and fractal dimension of fissures conformed to a quadratic polynomial.

The reliability of the model was verified by comparing the test results with an established macroscopic-mesoscopic damage model. Our results described the mechanism of macroscopic elastoplastic deformation caused by mesoscopic textural changes in red-bed soft rocks and provided a theoretical basis for the damage evolution of these rocks.

Funding

The research is supported by the National Natural Science Foundation of China (NSFC) (Grant Numbers: 42293354, 42293351, 42293355, 42277131, 41977230, 42293350).

References

Abd Rahman, N., Foong, L.K., Lewis, R.W. and Nazir, R. (2018), "Laboratory investigation of LNAPL migration in double-porosity soil under fractured condition using digital image analysis", *Transport. Porous Med.*, **125**(3), 521-542. https://doi.org/10.1007/s11242-018-1135-x.

An, D., Baik, S.I., Pan, S.Y., Zhu, M.F., Isheim, D., Krakauer, B.W. and Seidman, D.N. (2019), "Evolution of microstructure and carbon distribution during heat treatments of a dual-phase steel: Modeling and atom-probe tomography experiments", *Metall. Mater. Trans. A*, **50**(1), 436-450. https://doi.org/10.1007/s11661-018-4975-7.

Aubertin, M. and Simon, R. (1997), "A damage initiation criterion for low porosity rocks", *Int. J. Rock Mech. Min. Sci.*, **34**(3), 17.e1-17.e15. https://doi.org/10.1016/S1365-1609(97)00145-7.

Benavente, D., Martínez-Martínez, J., Cueto, N. and García-del-Cura, M.A. (2007), "Salt weathering in dual-porosity building dolostones", *Eng. Geol.*, **94**(3), 215-226. https://doi.org/10.1016/j.enggeo.2007.08.003.

Bour, O., Davy, P., Darcel, C. and Odling, N. (2002), "A statistical scaling model for fracture network geometry, with validation on a multiscale mapping of a joint network (Hornelen Basin, Norway)", *J. Geophys. Res.-Solid Earth*, **107**(6), 12. https://doi.org/10.1029/2001jb000176.

Bruning, T., Karakus, M., Nguyen, G.D. and Goodchild, D. (2018), "Experimental study on the damage evolution of brittle rock under triaxial confinement with full circumferential strain control", *Rock Mech. Rock Eng.*, **51**(11), 3321-3341. https://doi.org/10.1007/s00603-018-1537-7.

Chen, Y.R.X. and Luo, Y.L. (2018), "Analysis of paths and sources of moisture for the South China rainfall during the presummer rainy season of 1979-2014", *J. Meteorol. Res-Prc.*, **32**(5), 744-757. https://doi.org/10.1007/s13351-018-8069-7.

Chen, Z.Q., He, C., Ma, G.Y., Xu, G.W. and Ma, C.C. (2019), "Energy damage evolution mechanism of rock and its application to brittleness evaluation", *Rock Mech. Rock Eng.*, **52**(4), 1265-1274. https://doi.org/10.1007/s00603-018-1681-0.

Elsworth, D. and Bai, M. (2020), *Continuum representation of coupled flow-deformation response of dual porosity media*, Mechanics of Jointed and Faulted Rock.

Fischer, T., Gemmer, M., Liu, L.L. and Su, B.D. (2012), "Change-points in climate extremes in the Zhujiang River Basin, South China, 1961-2007", *Climatic Change*, **110**(3-4), 783-799. https://doi.org/10.1007/s10584-011-0123-8.

Lemaître J. and Chaboche J.-L. (1990), *Mechanics of solid materials*, Cambridge University Press, Cambridge.

Li, H., Yang, D.M., Zhong, Z.L., Sheng, Y. and Liu, X.R. (2018a), "Experimental investigation on the micro damage evolution of chemical corroded limestone subjected to cyclic loads", *Int. J. Fatigue*, **113**, 23-32. https://doi.org/10.1016/j.ijfatigue.2018.03.022.

Li, Y.Y., Zhang, S.C. and Zhang, X. (2018b), "Classification and fractal characteristics of coal rock fragments under uniaxial cyclic loading conditions", *Arab. J. Geosci.*, **11**(9). https://doi.org/10.1007/s12517-018-3534-2.

Liang, Y.J. (2016), "Rock fracture skeleton tracing by image processing and quantitative analysis by geometry features", *J. Geophys. Eng.*, **13**(3), 273-284. https://doi.org/10.1088/1742-2132/13/3/273.

Liu, H.Z., Xie, H.Q., He, J.D., Xiao, M.L. and Zhuo, L. (2017), "Nonlinear creep damage constitutive model for soft rocks", *Mech. Time-Depend. Mat.*, **21**(1), 73-96. https://doi.org/10.1007/s11043-016-9319-7.

Liu, S.W., Wan, J.H., Zhou, C.Y., Liu, Z. and Yang, X. (2020), "Efficient beam-column finite-element method for stability design of slender single pile in soft ground mediums", *Int. J. Geomech.*, **20**(1). https://doi.org/10.1061/(Asce)Gm.1943-5622.0001542.

Liu, T.Y., Cao, P. and Lin, H. (2014), "Damage and fracture evolution of hydraulic fracturing in compression-shear rock cracks", *Theor. Appl. Fract. Mech.*, **74**, 55-63. https://doi.org/10.1016/j.tafmec.2014.06.013.

Liu, W., Niu, S., Tang, H. and Zhou, K. (2021), "Pore structure evolution during lignite pyrolysis based on nuclear magnetic resonance", *Case Studies in Therm. Eng.*, **26**, 101125. https://doi.org/10.1016/j.csite.2021.101125.

Margherita, Z., Claudio, C., Laura, E. and Alessandra, N. (2018), "A risk assessment proposal for underground cavities in Hard Soils-Soft Rocks", *Int. J. Rock Mech. Min. Sci.*, **103**, 43-54. https://doi.org/10.1016/j.ijrmms.2018.01.024.

Nejati, H.R. and Ghazvinian, A. (2014), "Brittleness effect on rock fatigue damage evolution", *Rock Mech. Rock Eng.*, **47**(5), 1839-1848. https://doi.org/10.1007/s00603-013-0486-4.

Nishiyama, S., Ohnishi, Y., Ito, H. and Yano, T. (2014), "Mechanical and hydraulic behavior of a rock fracture under shear deformation", *Earth. Planets Space*, **66**. https://doi.org/10.1186/1880-5981-66-108.

Pan, P.Z., Su, F.S., Chen, H.J., Yan, S.L., Feng, X.T. and Yan, F. (2015), "Uncertainty analysis of rock failure behaviour using an integration of the probabilistic collocation method and elasto-plastic cellular automaton", *Acta Mech. Solida Sin.*, **28**(5), 536-555. https://doi.org/10.1016/S0894-9166(15)30048-3

Ping, C., Wen, Y.D., Wang, Y.X., Yuan, H.P. and Yuan, B.X. (2016), "Study on nonlinear damage creep constitutive model for high-stress soft rock", *Environ. Earth. Sci.*, **75**(10). https://doi.org/10.1007/s12665-016-5699-x.

Wang, C.L., Li, C.F., Chen, Z., Liao, Z.F., Zhao, G.M., Shi, F. and Yu, W.J. (2020a), "Experimental investigation on multi-parameter classification predicting degradation model for rock failure using Bayesian method", *Geomech. Eng.*, **20**(2), 113-120. https://doi.org/10.12989/gae.2020.20.2.113.

Wang, J.J., Ma, D., Li, Z.H., Huang, Y.L. and Du, F. (2022), "Experimental investigation of damage evolution and failure criterion on hollow cylindrical rock samples with different bore diameters", *Eng. Fract. Mech.*, **260**. https://doi.org/10.1016/j.engfracmech.2021.108182.

Wang, Y., Gao, S.H., Li, C.H. and Han, J.Q. (2020b), "Investigation on fracture behaviors and damage evolution modeling of freeze-thawed marble subjected to increasing-amplitude cyclic loads", *Theor. Appl. Fract. Mech.*, **109**. https://doi.org/10.1016/j.tafmec.2020.102679.

Wei, W., Hong, L.J. and Fei, S.P. (2014), "Analyses on CT image of gray rock uniaxial compressive failure process based on MATLAB", *Applied Decisions in Area of Mechanical Engineering and Industrial Manufacturing*, **577**, 1083-1086. https://doi.org/10.4028/www.scientific.net/AMM.577.1083.

Wu, H., Ji, Y.L., Liu, R., Zhang, C.L. and Chen, S. (2018), "Pore structure and fractal characteristics of a tight gas sandstone: A case study of Sulige area in the Ordos Basin, China", *Energ Explor Exploit*, **36**(6), 1438-1460. https://doi.org/10.1177/0144598718764750

Xie, H.P., Li, L.Y., Ju, Y., Peng, R.D. and Yang, Y.M. (2011), "Energy analysis for damage and catastrophic failure of rocks", *Sci. China Technol. Sc*, **54**: 199-209. https://doi.org/10.1007/s11431-011-4639-y

Xie, X., Su, D., Li, X. and Hu, H. (2021), "Research on red-bed soft rock engineering properties and foundation appraisement of construction engineering in Guangzhou", *IOP Conference Series: Earth Environmental Science and Technology*, **768**(1), 012162. https://doi.org/10.1088/1755-1315/768/1/012162.

Yan, F., Feng, X.T., Lv, J.H., Pan, P.Z. and Li, S.J. (2018), "Continuous-discontinuous cellular automaton method for cohesive crack growth in rock", *Eng. Fract. Mech.*, **188**, 361-380. https://doi.org/10.1016/j.engfracmech.2017.09.007.

Yan, F., Feng, X.T., Pan, P.Z. and Li, S.J. (2014), "A continuous-discontinuous cellular automaton method for cracks growth and coalescence in brittle material", *Acta Mech. Sinica-Prc.*, **30**(1), 73-83. https://doi.org/10.1007/s10409-014-0002-4.

Zhang, L.M., Cui, C.Y., Ma, X.P., Sun, Z.X., Liu, F. and Zhang, K. (2019), "A fractal discrete fracture network model for history matching of naturally fractured reservoirs", *Fractals*, **27**(1). https://doi.org/10.1142/S0218348x19400085.

Zhang, W. and Cai, Y. (2010), *Continuum Damage Mechanics and Numerical Applications*, Zhejiang University Press.

Zhang, Y.T., Ding, X.L., Huang, S.L., Wu, Y.J. and He, J. (2020), "Strength degradation of a natural thin-bedded rock mass subjected to water immersion and its impact on tunnel stability", *Geomech. Eng.*, **21**(1), 63-71. https://doi.org/10.12989/gae.2020.21.1.063.

Zhao, H.B., Zhang H., Li H.H., Wang F.H. and Zhang M. (2017), "Formation and fractal characteristics of main fracture surface of red sandstone under restrictive shear creep", *Int. J. Rock Mech. Min. Sci.*, **98**, 181-190. https://doi.org/10.1016/j.ijrmms.2017.07.011.

Zhao, Y. (2010), *Multi field coupling in porous media and its engineering response*, Science Press, Beijing.

Zhou, C., Cui, G., Yin, H., Yu, L., Xu, G., Liu, Z. and Zhang, L. (2021), "Study of soil expansion characteristics in rainfall-induced red-bed shallow landslides: Microscopic and macroscopic perspectives", *PLoS One*, **16**(1), e0246214. https://doi.org/10.1371/journal.pone.0246214.

Zhou, C.Y., Yu, L., You, F.F., Liu, Z., Liang Y.H. and Zhang L.H. (2020), "Coupled Seepage and Stress Model and Experiment Verification for Creep Behavior of Soft Rock", *Int J Geomech*, **20**(9). https://doi.org/10.1061/(Asce)Gm.1943-5622.0001774

Zhou, C.Y. and Zhu, F.X. (2010), "An elasto-plastic damage constitutive model with double yield surfaces for saturated soft rock", *Int. J. Rock Mech. Min. Sci.*, **47**(3), 385-395. https://doi.org/10.1016/j.ijrmms.2010.01.002.

GC